scientific reports

Check for updates

OPEN

AAV-IKV mediated expression of decorin inhibits EMT and fibrosis in a murine model of Glaucoma and AAV-IKV transduction in Non-Human Primates

Pushpa Rao[1], Manish Mishra[1], Siobhan M. Cashman[1], David S. Walton[2] & Rajendra Kumar-Singh[1]✉

Primary open angle glaucoma (POAG) and infantile aphakic glaucoma (IAG) are significant contributors of vision loss in adults and infants respectively. Both indications are associated with fibrosis of the trabecular meshwork (TM) that attenuates aqueous humor outflow, elevated intraocular pressure (IOP) and retinal ganglion cell (RGC) death. Transforming growth factor β2 (TGFβ2) is implicated in epithelial to mesenchymal transition (EMT) in both POAG and IAG. A major regulator of TGFβ2 is decorin, a proteoglycan whose expression is reduced in glaucoma patients. In this study we demonstrate highly efficient infection of the murine anterior chamber including ciliary body, corneal stroma, TM and corneal nerves using the adeno-associated virus (AAV) vector AAV-IKV. Intracameral injection of AAV-IKV expressing a constitutively active TGFβ2 (AAV-IKV-TGFβ2^{CS}) led to fibrosis of the TM in mice and a subsequent increase in IOP and RGC death, modeling pathophysiological features of POAG and IAG. Expression of human decorin from an AAV-IKV vector (AAV-IKV-Decorin) attenuated fibrosis, IOP and RGC death in AAV-IKV-TGFβ2^{CS} injected mice, suggesting that AAV-IKV-Decorin may function as a therapy for POAG and IAG respectively. Finally, intracameral injection of an AAV-IKV-GFP vector in a non-human primate led to expression of GFP in the cornea without any discernible toxicity.

Primary open angle glaucoma (POAG) in adults is the most common cause of irreversible blindness with a global prevalence of approximately 76 million individuals[1]. In addition, approximately 30,000 infants are born each year with cataract and secondary glaucoma following cataract surgery is considered the most sight-threatening complication of pediatric cataract care[2,3].

The cardinal and irreversible features of glaucoma include the loss of retinal ganglion cells (RGCs) and their axons that form the optic nerve[4,5]. The major risk factor associated with glaucoma is elevated intra ocular pressure (IOP)[4,5]. The causal link between elevated IOP and loss of RGCs is not completely understood, but interventions such as drugs or surgery that alleviate IOP have been found to attenuate progression towards blindness[4,5].

The ciliary body continuously produces aqueous humor, which exits the eye via the trabecular meshwork[4,5]. Accumulation of extracellular matrix deposits in the trabecular meshwork can impede drainage of aqueous humor, resulting in an increase in IOP[4,5]. Almost all drugs or surgical interventions for the treatment of glaucoma target either the production of aqueous humor by the ciliary body, or enhance the flow of aqueous humor through the trabecular meshwork[6,7]. Despite the availability of such drugs, glaucoma continues to be a significant cause of visual impairment and thus, there is an unmet clinical need for improved strategies to regulate IOP in glaucoma.

Studies on the genetics of glaucoma reveals a significantly complex and heterogenous disorder[8]. However, studies of aqueous or vitreous humor acquired from glaucoma patients during surgical intervention point to some key molecular pathways that may play central roles in the pathophysiology of disease irrespective of the genetic heterogeneity in glaucoma. Specifically, aqueous or vitreous humor from glaucoma patients has been found to contain elevated levels of Transforming Growth Factor β2 (TGFβ2)[9–17]. TGFβ2 is known to play an

[1]Department of Developmental, Molecular and Chemical Biology, Tufts University School of Medicine, MABoston, United States. [2]Department of Ophthalmology, Harvard Medical School, MABoston, United States. ✉email: Rajendra.Kumar-Singh@tufts.edu

important role in the metabolism of extracellular matrix (ECM) and epithelial to mesenchymal transition (EMT) to fibroblasts[18,19]. Thus, elevated TGFβ2 may play an important role in ECM remodeling and fibrosis at the trabecular meshwork. EMT is known to result in an increase in alpha smooth muscle actin (α-SMA) and coincidentally, increased expression of α-SMA has been documented in the aqueous humor of glaucoma patients[14]. In children, early lensectomy is believed to result in a tsunami of lens epithelial cells onto the anterior surface of the iris and the trabecular meshwork. Previously, it has been shown that TGFβ2 is a key player in EMT of lens epithelial cells[20]and we have proposed a hypothesis for the role of TGFβ2 in the pathogenesis of IAG[21].

A key negative regulator of TGFβ2 is the small leucine rich proteoglycan decorin[22]. Aqueous humor from glaucoma patients has been found to have reduced levels of decorin relative to 'normal' individuals[14,23]. Furthermore, anti-glaucoma medications have been found to lower decorin and alter profibrotic proteins including TGFβ2 in human tenon's fibroblasts[24]. These and other observations collectively suggest that the TGFβ2-decorin axis may play a significant role in the pathophysiology, and accordingly, the treatment of glaucoma.

The TGFβ2-decorin axis has recently been studied in animal models of glaucoma. Mice in which the decorin gene has been deleted exhibit a significant increase in IOP[23]. Loss of decorin also resulted in loss of optic nerve axons and morphological changes in the glial lamina: typical features observed in glaucoma patients[23]. Furthermore, injection of TGFβ2 into the eyes of rats has been found to effect an increase in IOP, that could be subsequently inhibited by injections of decorin[25]. In addition, adenovirus mediated gene transfer of TGFβ2 in mice or rats has been found to result in an increase in IOP and lead to reduced outflow of aqueous humor through the trabecular meshwork[26]. Open-angle infantile aphakic glaucoma is associated with lensectomy and is believed to be caused by the release of lens epithelial cells during cataract surgery that undergo TGFβ2-driven EMT at the trabecular meshwork[20]. Thus, while primary open angle and infantile aphakic glaucoma likely have a different origin of EMT and fibrosis at the trabecular meshwork, the TGFβ2-decorin axis may play a central role in both these related indications.

Glaucoma is a chronic disease needing treatment for long periods of time. The ocular surface poses significant barriers to drugs targeting the trabecular meshwork and 80 to 90% of drug applied topically to the eye drains through the lacrimal ducts[27]. Some drugs that are effective in glaucoma may have significant systemic consequences[28]. An alternative approach for the treatment of glaucoma is gene therapy, whereby continuous local production of a therapeutic may overcome the above limitations of topically applied drugs to the eye. The majority of preclinical gene therapy studies in the field of glaucoma have targeted preservation of RGCs through the use of signaling neuroprotective molecules[29]. However, such approaches do not address the primary pathophysiology in disease.

One challenge in gene therapy targeting the trabecular meshwork is the limited availability of potent adeno-associated virus (AAV) vectors for the trabecular meshwork. Recently, we have described a novel AAV referred to as AAV-IKV that can deliver transgenes to the outer retina following intravitreal injection[30]. Infection of retinal cells by AAV-IKV could be significantly enhanced through the use of a chaperone termed Nuc1[30,31]. In the current study we address whether AAV-IKV can infect cells of the anterior chamber including ciliary body, trabecular meshwork and cornea following intracameral injection. Subsequently, we investigate whether AAV-IKV mediated gene transfer of human TGFβ2 may be utilized to model pathophysiological aspects of glaucoma and we further investigate whether such a model may be utilized to evaluate AAV-IKV driven expression of decorin as a potential gene therapy for glaucoma. Finally, we address whether AAV-IKV coupled with Nuc1 is tolerated in non-human primate (NHP) eyes as a first step towards clinical development of a gene therapy for glaucoma.

Materials and methods

Animals

Six- to eight -week-old male C57BL/6 mice were purchased from The Jackson Laboratory (Bar Harbor, ME) and housed in our Institutional Animal Care and Use Committee (IACUC) approved animal facility at Tufts University School of Medicine. Animals were housed under a 12 h light/dark cycle. This study was carried out in accordance with the Statement for the Use of Animals in Ophthalmic and Vision Research, set out by the Association of Research in Vision and Ophthalmology (ARVO). Studies are reported in accordance with ARRIVE guidelines (https://arriveguidelines.org).

A study in African green monkey (*Chlorocebus sabaeus*) was conducted in compliance with ARVO Statement for the Use of Animals in Ophthalmic and Vision Research at the St. Kitts Biomedical Research Foundation. Monkeys were drug-naïve and humanely procured from the healthy wild population. Monkeys were observed twice daily in their home cages, assessing for behavioral changes and overall well-being. Additional monitoring was conducted during scheduled ophthalmic examinations. Animals were placed in single-cage housing throughout the study following approval from the IACUC.

Four monkeys were treated with anthelmintics to eliminate intestinal parasite burden and were observed in quarantine for a minimum of 4 weeks prior to screening for study enrollment. All monkeys underwent a minimum of 7 days acclimation to study housing prior to in-life initiation. Prior to study enrollment, a clinical exam was performed on the four monkeys. If healthy by these criteria, monkeys went through ophthalmic screening to identify an optimal animal for study enrollment. Baseline ophthalmic exam included tonometry, slit lamp biomicroscopy, fundoscopy, color fundus photography (CFP), fluorescence fundus photography, and optical coherence tomography (OCT) as described below.

General assessment of the monkeys was conducted a minimum of twice daily and during any sedation or restraint interval to confirm good health and identify abnormalities suggestive of adverse response to treatment.

Generation of AAV constructs

The AAV-IKV capsid as well as the Nuc1 chaperone, both utilized in this study have been described by us previously[30,31]. Methods to construct, amplify and purify AAV-IKV and an AAV-IKV expressing GFP (AAV-IKV-GFP) have also been described previously[30]. Specific to this study, an AAV-IKV vector containing a constitutively active TGFβ2 was constructed by mutating cysteine at positions 226 and 228 to serine of the human TGFβ2 propeptide (NP_003229) and replacing the GFP in AAV-IKV-GFP with this mutated TGFβ2, hereafter the construct being referred to as AAV-IKV-TGFβ2^{CS}. Similarly, a construct expressing human decorin (NM_001920) was also constructed (AAV-IKV-Decorin). Similar to GFP, both human transgenes were expressed from a chicken β actin promoter.

Intracameral injections

Mice were anesthetized by intraperitoneal injections of a mixture containing 0.1 mg/g body weight Ketamine (Phoenix™, St Joseph, MO) and of 0.01 mg/g body weight Xylazine (Lloyed, Shenandoah, Iowa) followed by topical application of 0.5% proparacaine hydrochloride (Akorn Inc., Lake Forest, IL, USA) to dilate the pupil. Injections were performed by delivering a total volume of 1.5 µl/eye using a Hamilton glass micro-syringe (Hamilton company, NV, USA) fitted with a custom 33-guage 0.5 inch, point style 4 needle with 30° bevel. After injecting the sample into the anterior chamber, the needle was left in place for 30s to 1 min before the needle was withdrawn. Injections were administered unilaterally, while un-injected eyes served as a contralateral control. Except where indicated, mice were injected with 0.52×10^9 vector genomes of the respective recombinant AAV virus.

Anesthesia was achieved in NHP with intramuscular ketamine (8 mg/kg) and xylazine (1.6 mg/kg) to effect, and pupil dilation with topical 10% phenylephrine and/or 1% cyclopentolate. For intracameral injection, a speculum was placed in the eye to facilitate injections followed by a drop of proparacaine hydrochloride 0.5% and then 5% Betadine solution, and a rinse with sterile saline. Intracameral (IC) injection containing 1.225×10^{11} AAV-IKV-GFP vector genomes including 12.5 µg Nuc1 was performed using 31-gauge 0.5-inch long needle connected to 0.3-mL syringe. The needle was introduced through the temporal cornea ~ 2 mm anterior to the limbus without disturbing the intraocular structures. Following completion of the injection, the needle remained inserted for approximately 10 s to ensure dispersal of the test article. The animal then received subconjunctival 50 µl of 40 mg/mL triamcinolone treatment. Following the injection, a topical triple antibiotic neomycin, polymyxin, bacitracin ophthalmic ointment was administered.

Tissue processing and immunostaining

Eyes were enucleated at the end of the study from the respective groups and incubated in a fixative comprising 4% paraformaldehyde (Electron Microscopy Sciences, 15735–50 S) at 4 °C, overnight. The next day the eyes were washed with PBS and transferred into 15% sucrose solution (in 0.1 M sodium phosphate solution, pH 7.4, Boston bioproducts, BB-149) for 5–6 h at 4 °C and subsequently transferred into 30% sucrose solution for overnight incubation at 4 °C. The next day, eyes were processed to snap freeze using O.C.T compound (Tissue Tek, 4583). Cryosections of 14 µm were incubated in either 2% BSA + 0.3% Triton X-100 or in 6% normal goat serum + PBS-Triton X-100 for 1 h at room temperature followed by incubation with a 1:200 dilution of primary antibody at 4 °C overnight. Detection was performed by incubation with a secondary Cy3-conjugated antibody for 1 h at room temperature. Imaging of stained sections was performed using an Olympus IX51 microscope and appropriate filters. Images were captured using a Retiga 2000r camera. The sources of antibodies and the dilutions used for staining are indicated below. Eyes for histology were fixed in Davidson's fixative solution (Electron Microscopy Sciences, 6413310). Paraffin embedding, sectioning and H/E staining was conducted by Tufts Comparative Pathology Services, Boston, MA. Images were acquired by using Olympus 1 × 51 microscope.

Antibodies used for immunohistochemistry

Antibody	Dilution	Catalog No	Supplier Name
α-SMA	1:200	C6198	Sigma Aldrich, MO
Fibronectin	1:200	ab45688	Abcam, MA
Brn3a	1:50	sc-8429	Santacruz,
TGFβ2	1:200	MAB73461	R & D systems, MN
Goat anti-rabbit cy3	1:500	111–165-003	Jackson ImmunoResearch, PA
Goat anti-rat cy3	1:500	A10522	Invitrogen, CA

IOP measurement

Baseline IOP was recorded from each mouse eye before administering intracameral injection and weekly once after intracameral injection in injected or uninjected eyes using an iCare Tonolab rebound tonometer (Icare, Finland), between 11AM and 2PM. This time range was maintained for each of the studies in order to avoid confounding results due to circadian variability in IOP[32]. Mice were anaesthetized before measuring IOP. Six rebound measurements were recorded with the tonometer measured from the central cornea to provide an average value of IOP (mm Hg). All IOP measurements were conducted following the manufacturer's recommendations. The standard deviation of six rebound measurements less than 2.5 (SD < 2.5) were considered

to ensure recording of accurate IOP value. The measurements were repeated if the above range was not initially met.

In NHPs, IOP measurements were collected using a TonoVet (iCare, Finland) tonometer set to the dog (d) calibration setting. The TonoVet rebound tonometer is well tolerated and required no additional local analgesia. Approximately 4 min after administration of anesthesia, when full sedation was achieved, monkeys were placed in a supine position in an IOP testing apparatus. Approximately one minute after supine positioning, three measurements were taken from each eye at each time point and the mean was used for IOP analysis.

Statistical analysis

Statistical analysis was performed using GraphPad Prism software (San Diego, CA). All *p*-values were determined by unpaired two-tailed parametric t test or nonparametric Mann–Whitney U test. One-way or Two-way ANOVA followed by Bonferroni's multiple comparison test was used to determine statistically significant differences when comparing the results of more than two or three independent groups. Differences were considered statistically significant as follows: $^{*}p \leq 0.05$, $^{**}p \leq 0.01$, $^{***}p \leq 0.001$, and $^{****}p \leq 0.0001$. Results are shown as the mean ± SEM.

Ophthalmic exams in Non-Human Primates

One monkey weighing 4.84 Kg of approximate age 9 to 11 years was selected for study. Eyes were examined by slit lamp at baseline and intervals up to completion of study (day 43 post intracameral injection) to confirm integrity of the ocular surface and general ocular health, broad ocular response to AAV-IKV-GFP and normal response to mydriatics (10% phenylephrine HCl and 1% cyclopentolate HCl). Ophthalmic imaging including color fundus, fluorescence fundus and OCT imaging were performed as described below to confirm any pathological response from AAV-IKV-GFP.

Anterior & fundus photography in Non-Human Primates

Color anterior and fundus imaging, and fluorescent anterior and fundus imaging were performed using a Topcon TRC-50EX retinal camera with Canon 6D digital imaging hardware and New Vision Fundus Image Analysis System software. For the color anterior and fundus photos, the following settings were applied: shutter speed (Tv) 1/25 sec, ISO 400 and Flash 18. For monochromatic anterior and fundus photos the following settings were applied: Tv 1/5 sec, ISO 400 and Flash 25. For fluorescent anterior and fundus images the following settings were applied: exciter and barrier filters engaged (480 nm exciter/525nm barrier filter), Tv 1/5 sec, ISO 3200 and Flash 300. Fluorescence photographs were qualitatively evaluated to define extent of GFP expression.

Optical coherence tomography in Non-Human Primates

Anterior and posterior segment optical coherence tomography (OCT) were performed oculus uturque (OU, both eyes) using a Heidelberg Spectralis OCT HRA plus or OCT system with eye tracking and HEYEX image capture and analysis software. An overall volume scan of the entire macula was performed at a dense scan interval. At the time of OCT measurement, the blue laser autofluorescence wide-field function of the Spectralis was used to obtain images of GFP expression in the retina and anterior chamber. When permitted by media clarity, the composite image function was employed to maximize the area of the retina that is captured in each image file.

Termination and eye collection in Non-Human Primates

Animals were terminated on Day 45 after review of Day 43 images and euthanized with sodium pentobarbital (25–30 mg/kg IV). Globes were enucleated after marking the 12:00 o'clock position with a limbal suture. Thereafter ~ 8 mm limbal incision was made, followed by trimming of excess orbital tissue with retention of the optic nerve. Globes were transferred to 4% paraformaldehyde solution (prepared in PBS) for 4 h at 4 °C and then thoroughly washed in PBS three times for 15 min each. Globes were then immersed in 30% sucrose solution (prepared in PBS) at 4 °C and processed as described above.

Results

AAV-IKV mediated gene delivery to the murine anterior segment

Dependent upon the serotype, intracamerally injected AAV infects primarily the corneal endothelium, stroma or trabecular meshwork[33]. Recently, we have shown that AAV-IKV can potently infect outer retinal cells following intravitreal injection[30]. AAV-IKV mediated infection of cells could be further enhanced when co-injected with a novel cell penetrating chaperon referred to as Nuc1[31]. In order to examine whether this same AAV-IKV/Nuc1 combination can infect cells in the anterior chamber, we injected 1.1×10^9 genome copies of a GFP-expressing AAV-IKV regulated by the chicken β actin promoter (AAV-IKV-GFP) with 1 µg Nuc1 intracamerally into adult C57BL/6J mice. Two weeks following injection, frozen anterior chamber sections were examined for expression of GFP. We detected strongly GFP-positive cells in the ciliary body, iris, cornea and lens (Fig. 1A). Closer examination revealed that GFP expression was in the corneal stroma, ciliary body and trabecular meshwork and some limited GFP expression was also observed in the corneal endothelium (Fig. 1B). Unexpectedly, we also documented presence of GFP in some of the corneal nerves (Fig. 1C). The pigment in the ciliary process obscured some of the GFP expression. Bright field images merged with GFP revealed punctate GFP in the pigmented ciliary process and iris, suggesting that there is potentially greater GFP-expression in these tissues than could be readily detected via fluorescence (Fig. 1D). We conclude that the AAV-IKV/Nuc1 combination can enable transgene delivery to a variety of cell types and locations in the anterior chamber of mice.

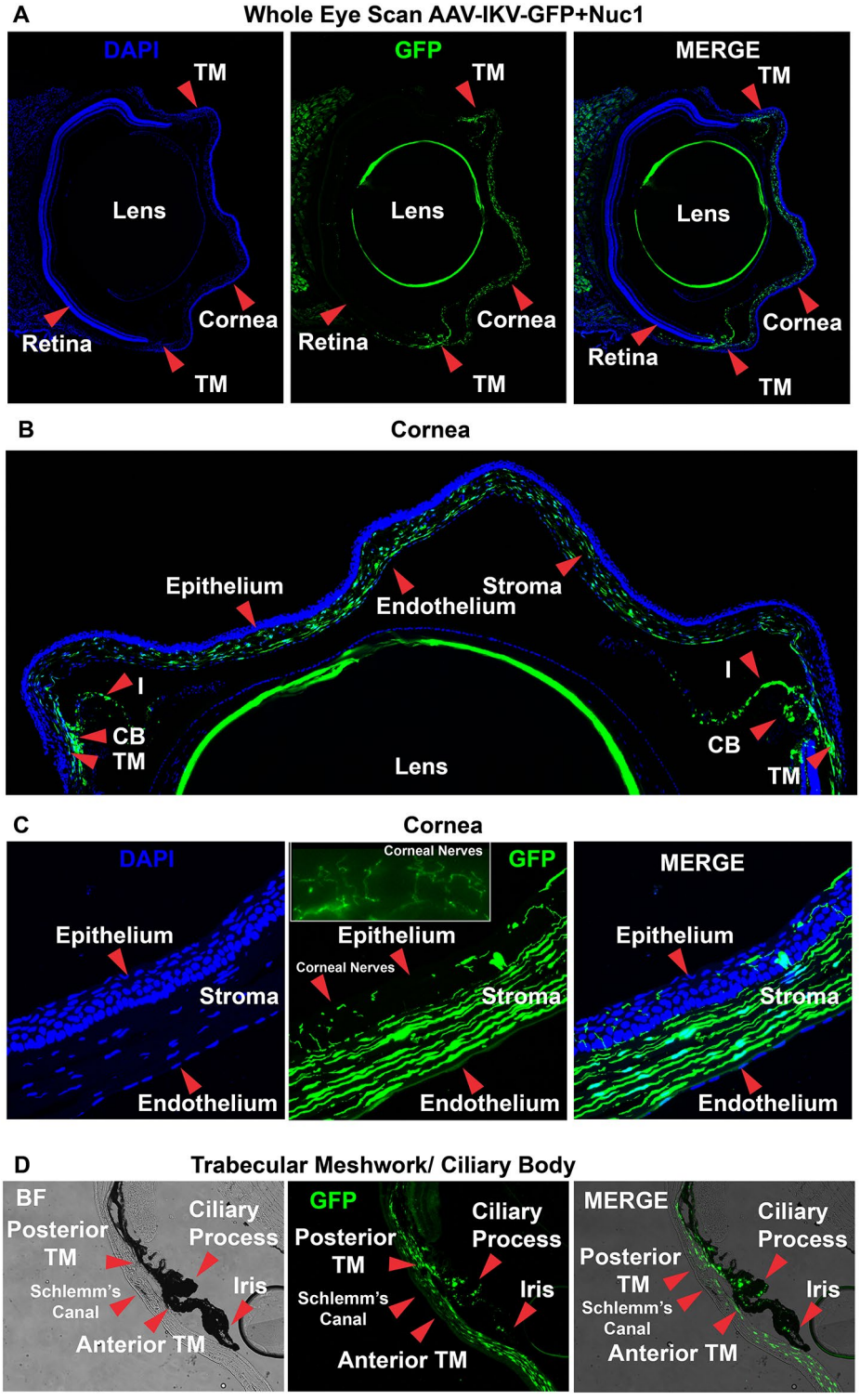

Fig. 1. AAV-IKV Mediated Gene Delivery to the Cornea and Trabecular Meshwork. (**A**) Imaging of whole eye sections from six-weeks old C57BL/6J mouse injected intracamerally with AAV-IKV-GFP indicating GFP expression in the endothelium, stroma and trabecular meshwork. (**B**) Higher power reveals that GFP expression is primarily in the corneal stroma, ciliary body and trabecular meshwork and some limited GFP expression is in the corneal endothelium. (**C**) GFP is also present in some of the corneal nerves. (**D**) Bright field images merged with GFP reveal punctate GFP in the pigmented ciliary process and iris. TM, Trabecular meshwork; CB, Ciliary Body; I, Iris; BF, Bright Field; GFP, green fluorescent protein channel.

TGFβ2 mediated increase in intraocular pressure

In order to investigate whether AAV mediated delivery of TGFβ2 can cause an increase in intra ocular pressure (IOP), we constructed a recombinant AAV-IKV expressing human TGFβ2 regulated by a chicken b actin promoter. The TGFβ2 cDNA was mutated such as to encode serine instead of cysteine at positions 226 and 228 in the TGFβ2 propeptide (NP_003229), hereafter the construct being referred to as AAV-IKV-TGFβ2^{CS}. These two mutations in TGFβ2 have been previously shown to result in a spontaneously active TGFβ2. We injected 1.47×10^9 genome units of AAV-IKV-TGFβ2^{CS} with 0.5 μg Nuc1 or a control vector without a cDNA (AAV-IKV-pA) intracamerally and TGFβ2 expression was measured in frozen anterior chamber sections by immunohistochemistry one week after injection. We found that relative to uninjected animals, AAV-IKV-TGFβ2^{CS} injected animals expressed significantly greater levels of TGFβ2 in the ciliary body and trabecular meshwork (Fig. 2A). We also noted a higher level of TGFβ2 in the ciliary body of AAV-IKV-pA injected animals relative to uninjected animals, but these levels were lower than that found in AAV-IKV-TGFβ2^{CS} injected animals, suggesting that some native TGFβ2 was upregulated as a consequence of either the AAV backbone or the injection procedure itself (Fig. 2A). We conclude that AAV-IKV-TGFβ2^{CS} elevates expression of TGFβ2^{CS} from the ciliary body and trabecular meshwork when injected intracamerally in mice.

Having confirmed that AAV-IKV-TGFβ2^{CS} could increase expression of TGFβ2^{CS} in the ciliary body and trabecular meshwork, we addressed whether such elevated TGFβ2^{CS} would result in increased IOP. We injected 0.52×10^9 AAV-IKV-TGFβ2^{CS} vector genomes supplemented with 0.5 μg Nuc1 peptide (hereafter, except where indicated, all viral injections contained 0.5 μg Nuc1) intracamerally into adult C57BL/6J mice. In a separate group of animals, as negative controls, we injected AAV-IKV-pA. Following injection, we measured intraocular pressure (IOP) in injected mice on a weekly basis, specifically, at days 8, 16, 23, 30, 37 and 44 post injection. We found that at all time points examined (Fig. 2B), there was a statistically significant increase in IOP in AAV-IKV-TGFβ2^{CS} injected eyes relative to AAV-IKV-pA injected eyes ($p<0.0001$, D8; $p=0.0095$, D16; $p<0.0001$, D23; $p<0.0001$, D30; $p=0.03$, D37; $p=0.001$, D44). Increase in IOP was rapid, detectable within one week after injection of AAV-IKV-TGFβ2^{CS}. We conclude that AAV-IKV-TGFβ2^{CS} injected mice may serve as a model for the testing of inhibitors of TGFβ2^{CS} mediated elevation of IOP.

In a separate group of animals, we examined the resulting IOP upon intracameral injection of 2X dose of AAV-IKV-TGFβ2 ^{CS}, specifically, 1.04×10^9 vector genomes. As anticipated, in this group of animals there was also a statistically significant increase in IOP relative to AAV-IKV-pA injected animals at all time points and the difference was greater than that seen with 0.52×10^9 AAV-IKV-TGFβ2^{CS} vector genomes (Fig. 2B). However, when comparing 1.04×10^9 with 0.52×10^9 vector genomes of AAV-IKV-TGFβ2^{CS}, we found a statistically significant increase in IOP at the higher dose at 3 of the 5 time points ($p=0.12$, D8; $p<0.0001$, D16; $p=0.03$, D23; $p=0.03$, D30; $p=0.24$, D37; $p=0.8866$, D44).

Furthermore, intracameral injection of AAV-IKV-pA did not result in a statistically significant change in IOP relative to uninjected animals at any time point (see below). Thus, we conclude that intracameral injection of AAV-IKV-TGFβ2^{CS} results in a significant increase in IOP in a dose dependent manner and that this increase is due to the expression of TGFβ2^{CS} and not the injection procedure or the recombinant AAV per se. Furthermore, the elevated IOP persists until at least day 44 post intracameral injection- the latest time point examined in this study.

TGFβ2^{CS} induces fibrosis at the trabecular meshwork

Extracellular matrix deposition at the trabecular meshwork is believed to be a major cause of elevated IOP in glaucoma patients. To examine whether AAV-IKV-TGFβ2^{CS} injected animals exhibited any significant fibrosis of the trabecular meshwork, we stained frozen sections from AAV-IKV-TGFβ2 ^{CS} injected animals for α- smooth muscle actin (α-SMA) at 44 days post injection. Staining for α-SMA was found to be significantly elevated at the trabecular meshwork (Fig. 3A). Staining for α-SMA was undetectable under the same conditions in uninjected animals (Fig. 3B). However, we also detected some low levels of α-SMA staining in AAV-IKV-pA injected animals relative to uninjected animals (Supplementary Fig. 1), suggesting that either the injection procedure, or AAV itself can contribute to some increase in α-SMA staining. However, the level of α-SMA staining associated with AAV-IKV-pA was substantially less than that associated with AAV-IKV-TGFβ2^{CS}. Thus, we conclude that the significantly elevated α-SMA staining in mice injected with AAV-IKV-TGFβ2^{CS} was largely associated with expression of TGFβ2^{CS}.

We also examined expression of fibronectin in these studies. We found that similar to α-SMA, there were elevated levels of fibronectin at the trabecular meshwork in AAV-IKV-TGFβ2^{CS} injected animals relative to uninjected animals. However, similar to α-SMA, there was a higher level of fibronectin staining in AAV-IKV-pA injected animals relative to uninjected animals (Supplementary Fig. 1B). Again, we conclude that the significantly elevated fibronectin staining in mice injected with AAV-IKV-TGFβ2^{CS} was largely associated with expression of TGFβ2^{CS}.

AAV-IKV mediated delivery of decorin inhibits AAV-IKV-TGFβ2^{CS} induced IOP

Decorin is a small leucine rich proteoglycan expressed in the eye. Decorin is known to be able to bind and sequester TGFβ2. In order to examine if human decorin could be expressed in the murine anterior segment, we injected 0.52×10^9 vector genomes of AAV-IKV-Decorin or AAV-IKV-pA intracamerally into six week old C57BL/6J mice and stained frozen sections after 7 days post injection for decorin. We found that whereas there was a detectable level of decorin in AAV-IKV-pA injected eyes in the ciliary body, there was a significantly higher level of decorin expression in AAV-IKV-Decorin injected eyes (Fig. 4A).

We next wished to examine whether expression of Decorin could inhibit AAV-IKV-TGFβ2^{CS} induced increase in IOP in mice. Thus, we injected either 0.52×10^9 AAV-IKV-TGFβ2^{CS} vector genomes intracamerally

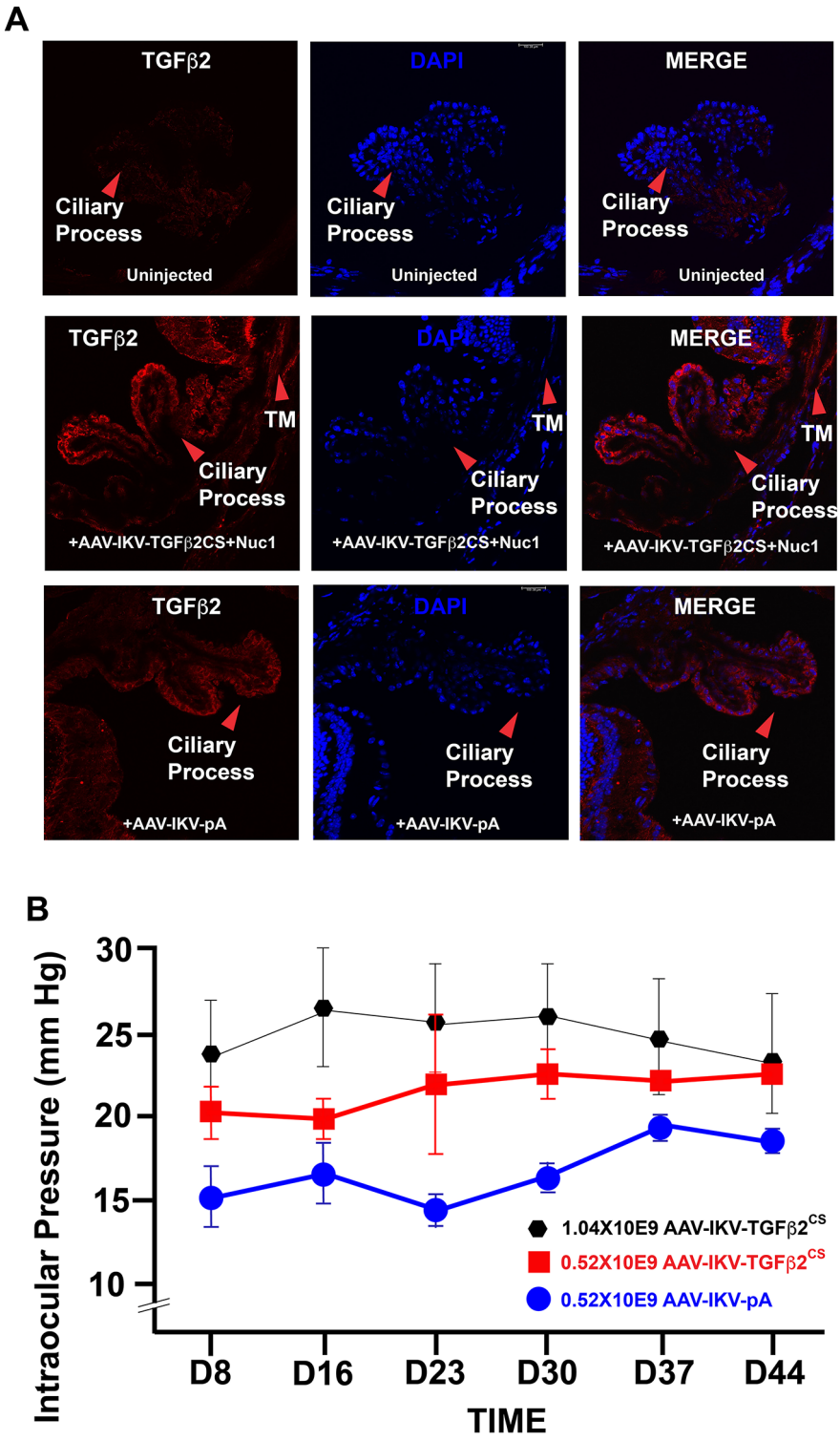

Fig. 2. TGFβ2 mediated increase in Intra Ocular Pressure. **(A)** TGFβ2 expression in frozen anterior chamber sections by immunohistochemistry approximately one week after infection with AAV-IKV-TGFβ2^{CS}. Relative to uninjected animals, AAV-IKV-TGFβ2^{CS} injected animals express significantly greater levels of TGFβ2 in the ciliary body and trabecular meshwork. Some TGFβ2 is elevated in AAV-IKV-pA injected animals as a consequence of either the AAV backbone or the injection procedure itself. (**B**) IOP increases within one week after injection of AAV-IKV-TGFβ2^{CS}. Intracameral injection of AAV-IKV-pA did not result in a statistically significant change in IOP relative to uninjected animals at any time point (see Fig. 4).

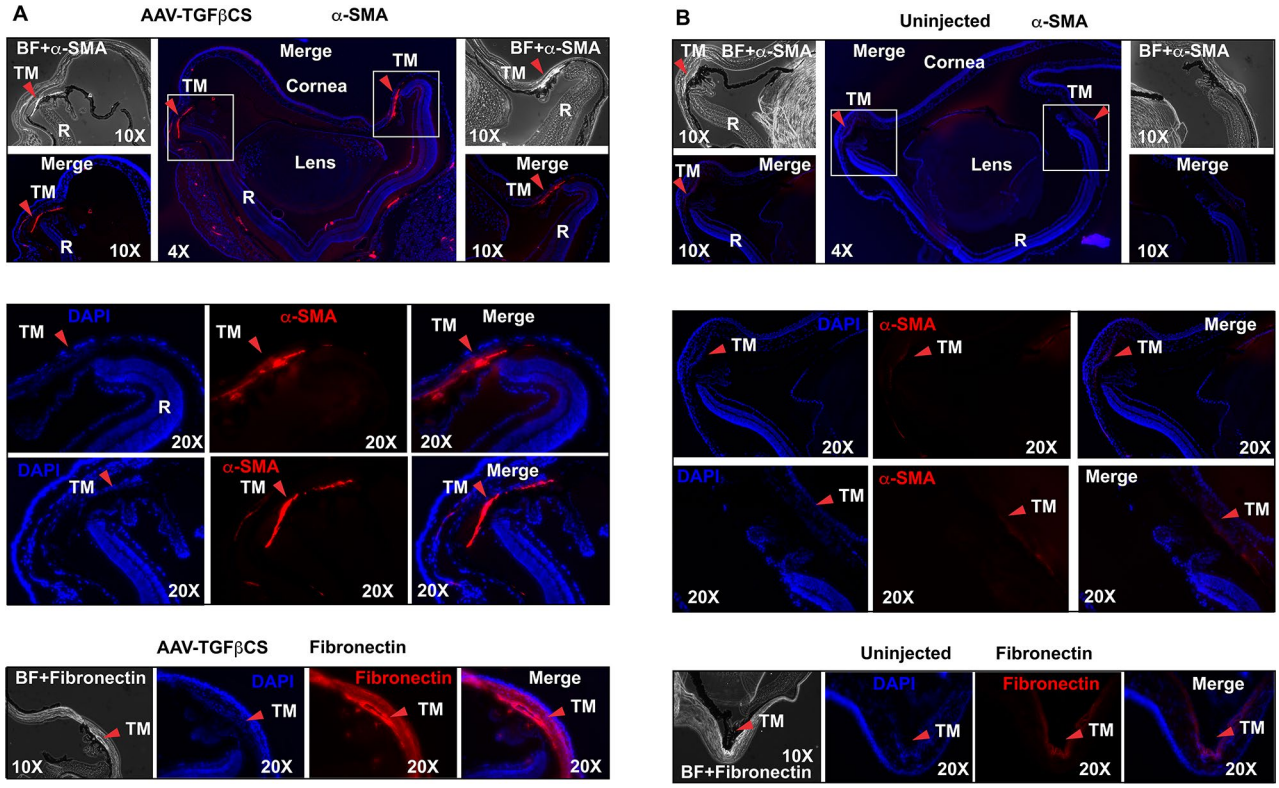

Fig. 3. TGFβ2^{CS} induces Fibrosis at the Trabecular Meshwork. (**A**) Frozen sections from AAV-IKV-TGFβ2 ^{CS} injected animals stained for α- smooth muscle actin (α-SMA) and fibronectin 44 days post injection. (**B**) Staining for α-SMA and fibronectin was undetectable under the same conditions in uninjected animals.

into adult C57BL/6J mice or in a separate group of animals we co-injected the same number of vector genomes of AAV-IKV-TGFβ2 ^{CS} with an equivalent dose of AAV-IKV-Decorin.

We found that while there was no statistically significant difference in IOP between the AAV-IKV-TGFβ2^{CS} and AAV-IKV-TGFβ2^{CS} + AAV-IKV-Decorin groups initially, i.e. at day 8 ($p = 0.13$) and day 16 ($p = 0.7$), there was a sustained lowering in IOP in AAV-IKV-TGFβ2^{CS} + AAV-IKV-Decorin injected group relative to the AAV-IKV-TGFβ2^{CS} injected group at all subsequent time points examined ($p < 0.0001$, D23; $p < 0.0001$, D30; $p = 0.016$, D37; $p = 0.005$, D44). Thus, we conclude that expression of Decorin results in a lowering of IOP in AAV-IKV-TGFβ2^{CS} animals but such reduction in IOP takes approximately two weeks to be statistically significantly different to AAV-IKV-TGFβ2^{CS} injected animals. The reduction in IOP was sustained until day 44, the latest time point examined in this study. Furthermore, IOP in animals injected with AAV-IKV-TGFβ2^{CS} + AAV-IKV-Decorin was statistically indistinguishable from IOP in uninjected animals (Fig. 4B), suggesting that after an initial two weeks, IOP was reduced and maintained at normal levels.

Decorin inhibits TGFβ2^{CS} induced fibrosis at the trabecular meshwork

Above, we found that intracameral injection of AAV-IKV-TGFβ2^{CS} with Nuc1 resulted in intense staining for α-SMA at the trabecular meshwork and in the ciliary body. We examined whether co-injection of AAV-IKV-Decorin with AAV-IKV-TGFβ2^{CS} would result in a reduced amount of fibrosis. We found that α-SMA as well as fibronectin staining was reduced at the trabecular meshwork in the presence of Decorin relative to both the AAV-IKV-TGFβ2^{CS} injected groups (Fig. 5) as well as AAV-IKV-pA groups (see Supplementary Fig. 1). We conclude that AAV-IKV mediated expression of decorin can significantly inhibit TGFβ2^{CS} mediated fibrosis at the trabecular meshwork.

Decorin inhibits IOP mediated retinal ganglion cell degeneration

The cardinal feature of glaucoma is retinal ganglion cell (RGC) degeneration as a consequence of elevated IOP. Loss of these cells is essentially the end stage of disease and the major irreversible factor contributing to visual impairment in glaucoma patients. With the knowledge that animals injected with AAV-IKV-Decorin counteract the activity of TGFβ2^{CS} and subsequently elevated IOP, we hypothesized that there may be a reduction in RGC death in AAV-IKV-TGFβ2^{CS} + AAV-IKV-Decorin injected animals. Thus, we stained RGCs with BRN3a in frozen sections from AAV-IKV-TGFβ2^{CS} and AAV-IKV-TGFβ2^{CS} + AAV-IKV-Decorin injected animals as well as uninjected or AAV-IKV-pA injected animals. We found that there was no statistically significant difference in BRN3a staining between uninjected and AAV-IKV-pA injected animals. However, there was a statistically significant greater number of RGCs in the AAV-IKV-TGFβ2^{CS} + AAV-IKV-Decorin injected group relative to

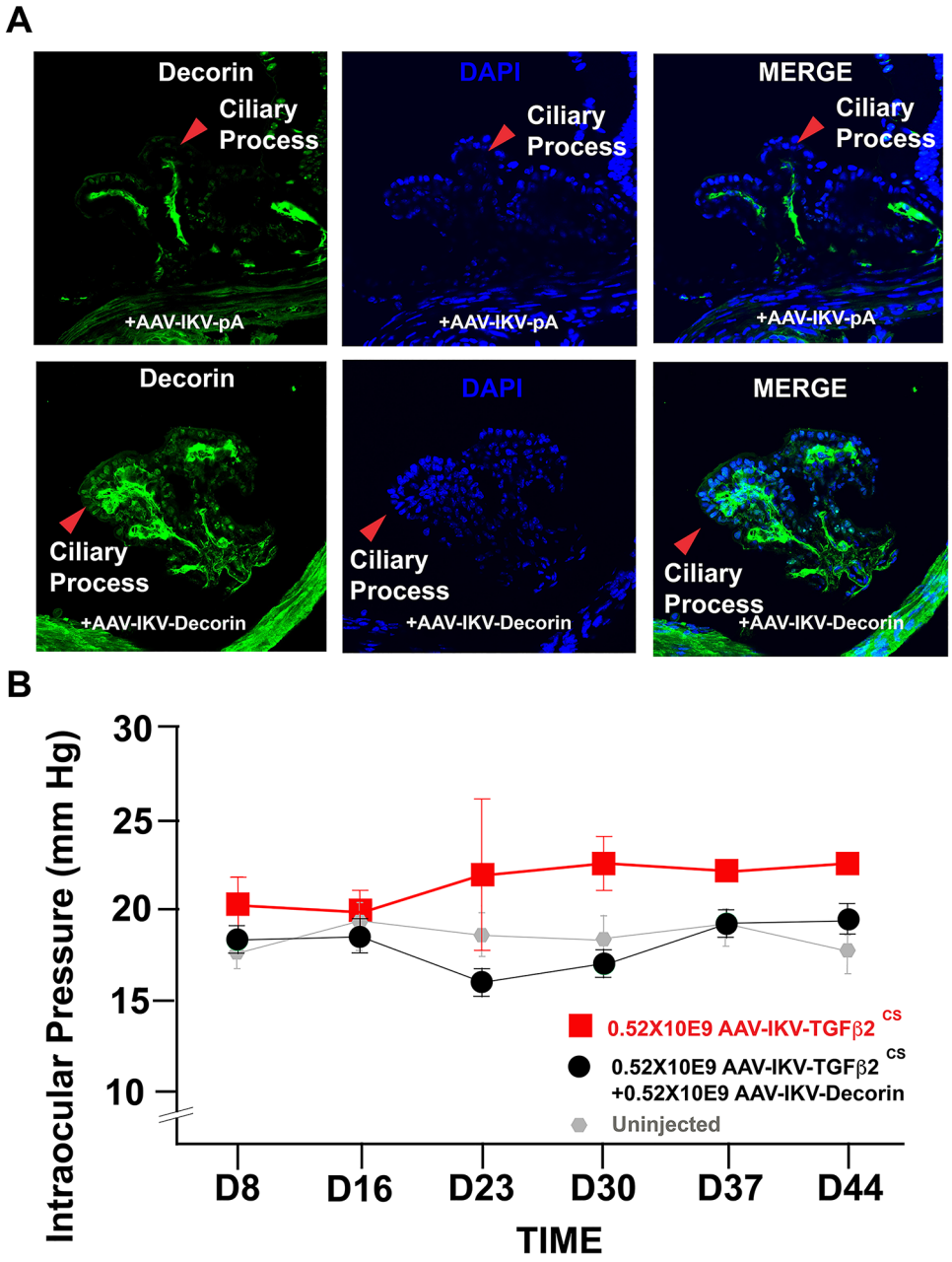

Fig. 4. AAV-IKV Mediated Delivery of Decorin Inhibits AAV-IKV-TGFβ2^{CS} induced IOP. (**A**) AAV-IKV-Decorin or AAV-IKV-pA injected intracamerally into six week old C57BL/6J mice and stained for decorin after 7 days post injection. Whereas there is a detectable level of decorin in AAV-IKV-pA injected eyes in the ciliary body, there is a significantly higher level of decorin expression in the AAV-IKV-Decorin injected eyes. (**B**) We found that while there was no statistically significant difference in IOP between the AAV-IKV-TGFβ2^{CS} and AAV-IKV-TGFβ2^{CS} + AAV-IKV-Decorin groups initially, i.e. at day 8 ($p = 0.13$) and day 16 ($p = 0.7$), there was a sustained lowering in IOP in AAV-IKV-TGFβ2^{CS} + AAV-IKV-Decorin injected group relative to the AAV-IKV-TGFβ2^{CS} injected group at all subsequent time points examined ($p < 0.0001$, D23; $p < 0.0001$, D30; $p = 0.016$, D37; $p = 0.005$, D44).

AAV-IKV-TGFβ2^{CS} injected animals ($p = 0.0322$) (Fig. 6). Thus, we conclude that expression of decorin can inhibit TGFβ2^{CS} mediated death of RGC.

AAV-IKV mediated gene delivery to the Non-Human primate cornea

Our results above suggest that use of AAV-IKV-Decorin for the treatment of glaucoma may be worth evaluating in a larger species of animal prior to consideration of testing in humans. Although conducting the studies described above in non-human primates (NHPs) is beyond the scope of the current study, as a critical first step

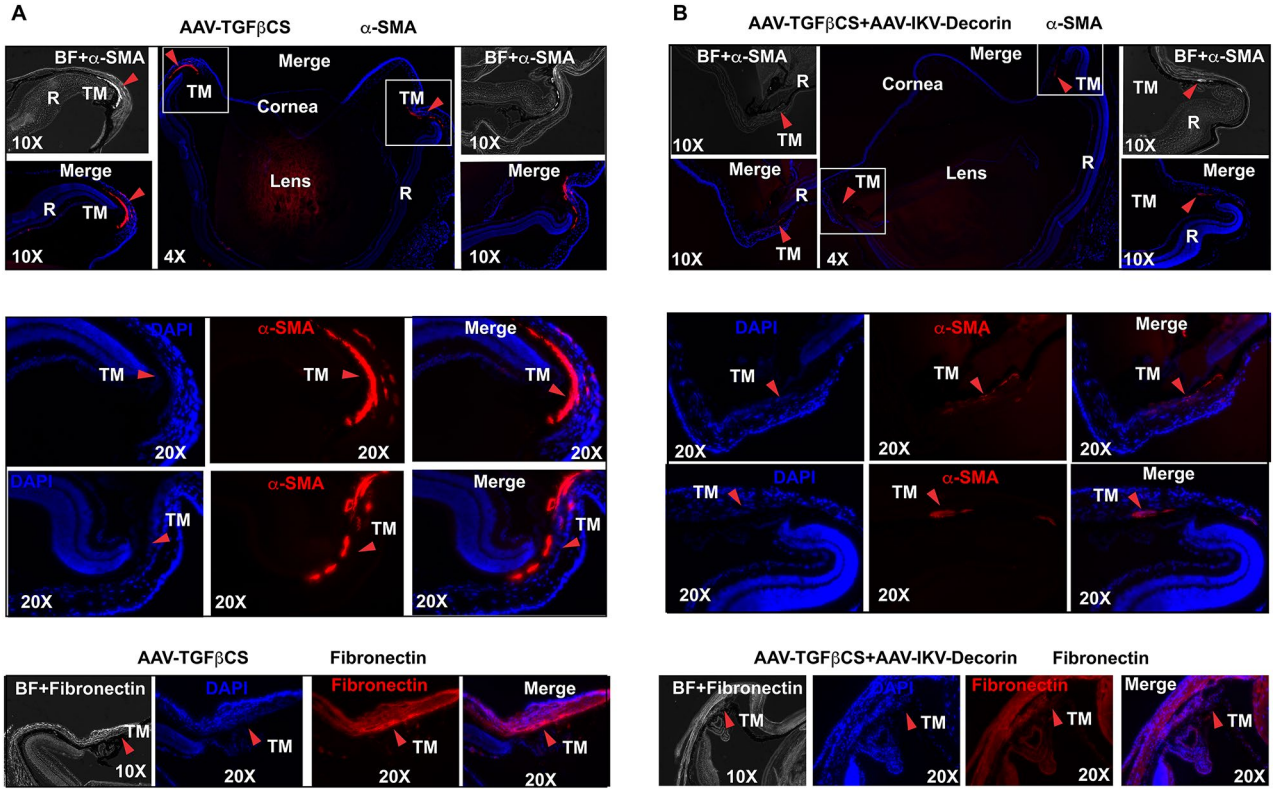

Fig. 5. Decorin Inhibits TGFβ2^{CS} induced Fibrosis at the Trabecular Meshwork. (**A**) Frozen sections from AAV-IKV-TGFβ2 ^{CS} injected animals stained for α- smooth muscle actin (α-SMA) and fibronectin 44 days post injection. (**B**) Staining for α-SMA and fibronectin was significantly less in AAV-IKV-TGFβ2^{CS} + AAV-IKV-Decorin injected groups.

we addressed whether AAV-IKV-GFP is capable of transducing NHP cornea via intracameral injection. We wished to further evaluate whether a non-GMP grade AAV-IKV-GFP and Nuc1 could be tolerated in NHPs.

A total of 1.225 × 10E11 AAV-IKV-GFP vector genomes including 12.5 µg Nuc1 were injected intracamerally in two eyes of one African green monkey (*Chlorocebus sabaeus*) weighing 4.84 Kg of approximate age 9 to 11 years. Color and fluorescence anterior and posterior photos were acquired 7 days prior to injection (injection defined as day 0, baseline) and at day 14 and 37 post injection. Additional parameters that were measured at day 14 and 37 included slit lamp, IOP and OCT. Body weights were measured 7 days prior to injection as well as day of injection and 4 days prior to end of study (day 41).

As anticipated, there was no detectable GFP fluorescence at baseline (Fig. 7A). However, at day 14 and day 37, punctate GFP fluorescence in live animals could be readily observed in both *oculus dexter* (OD, right eye) and *oculus sinister* (OS, left eye) (Fig. 7A arrowheads). Frozen sections collected at day 41 and examined by fluorescence microscopy revealed significant levels of GFP in the cornea (Fig. 7B). The IOP in OS and OD in AAV-IKV-GFP injected eyes did not differ significantly from baseline (Fig. 7C).

High resolution OCT imaging of cornea, sclera and anterior chamber angles of OS and OD revealed that AAV-IKV-GFP injected eyes at day 14 and day 37 were similar to baseline (Fig. 8D and Supplementary Fig. 2). Volume scans of OS and OD macula revealed an average thickness of the retina at day 14 and 37 also similar to baseline (Fig. 8D and Supplementary Fig. 2). High resolution OCT imaging of OS and OD retina of AAV-IKV-GFP injected eyes at day 14 and day 37 were also similar to baseline (Fig. 8D and Supplementary Fig. 2).

Anterior OS and OD fundus color as well as fluorescence fundus at day 14 and 37 were similar to baseline (Fig. 8). However, at day 40, there was some evidence of GFP expression in the fundus relative to baseline (Fig. 8). Finally, in AAV-IKV-GFP injected eyes the total clinical score (zero) comprising of but not limited to vitreous haze, retinal vasculitis, vitreous cell, lens opacity, anterior and posterior lens capsule deposit, iris exfoliation and synechia, aqueous flare, melanocytes, macrophages, corneal opacity, corneal vascular pannus and conjunctival congestion, swelling and discharge were all similar to baseline. In conclusion, our studies suggest that AAV-IKV-GFP coupled with Nuc1 is well tolerated in NHPs.

Discussion

In this study we have shown that AAV-IKV is a potent gene delivery vector for the anterior segment, including the ciliary body, cornea and trabecular meshwork. This AAV vector can efficiently deliver TGFβ2 to the anterior segment, resulting in an increase in intraocular pressure- a key feature observed in glaucoma and IAG patients. We have also shown that AAV-IKV delivered TGFβ2 induces fibrosis at the trabecular meshwork, again

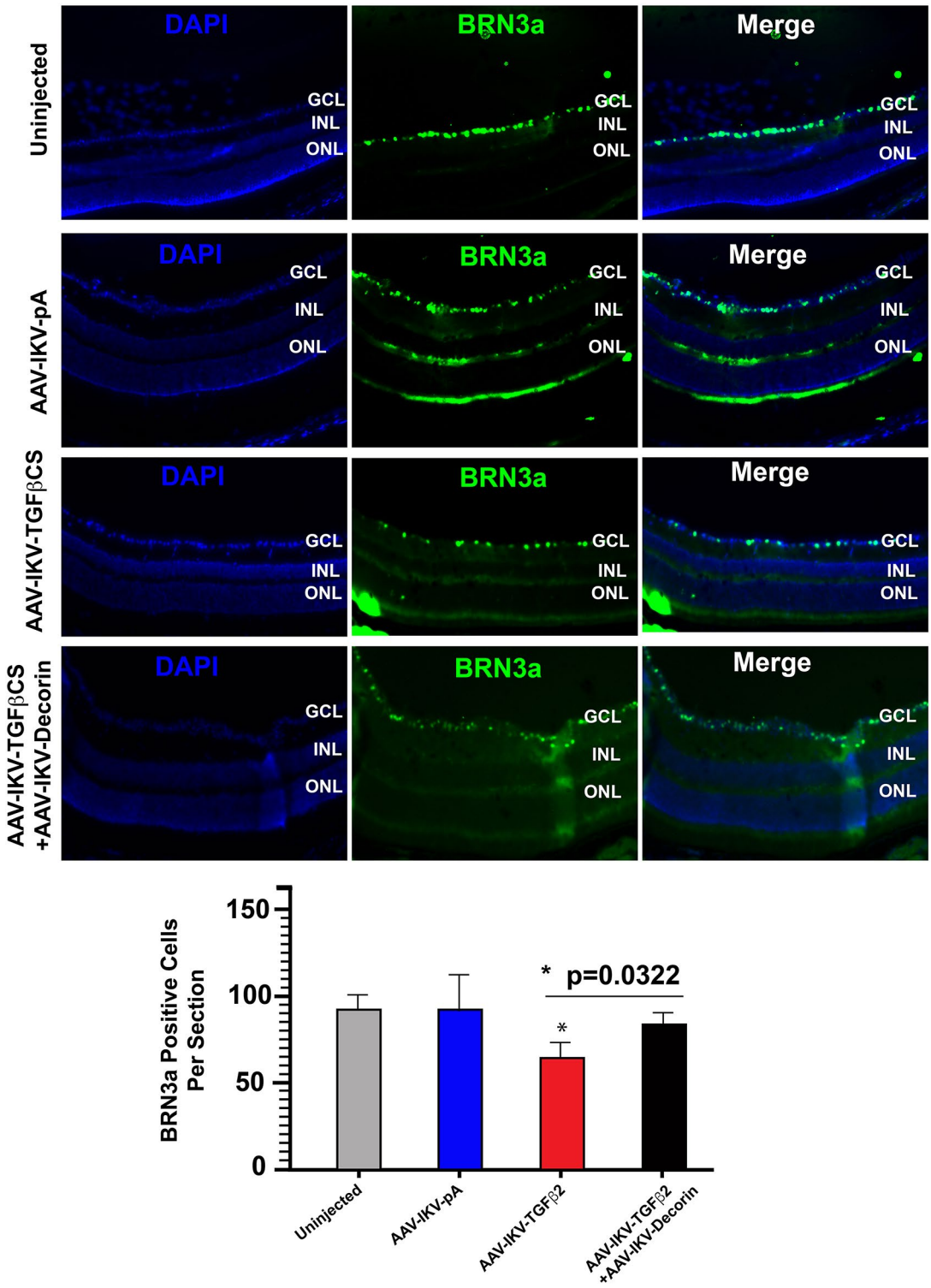

Fig. 6. Decorin Inhibits Retinal Ganglion Cell Death. Frozen retinal sections stained with BRN3a for quantitation of Retinal ganglion cells (RGCs) in AAV-IKV-TGFβ2^{CS} and AAV-IKV-TGFβ2^{CS} + AAV-IKV-Decorin injected groups as well as uninjected or AAV-IKV-pA injected animals. There was no statistically significant difference in BRN3a staining between uninjected and AAV-IKV-pA injected animals. However, there was a statistically significant greater number of RGCs in the AAV-IKV-TGFβ2^{CS} + AAV-IKV-Decorin injected group relative to AAV-IKV-TGFβ2^{CS} injected animals ($p = 0.0322$).

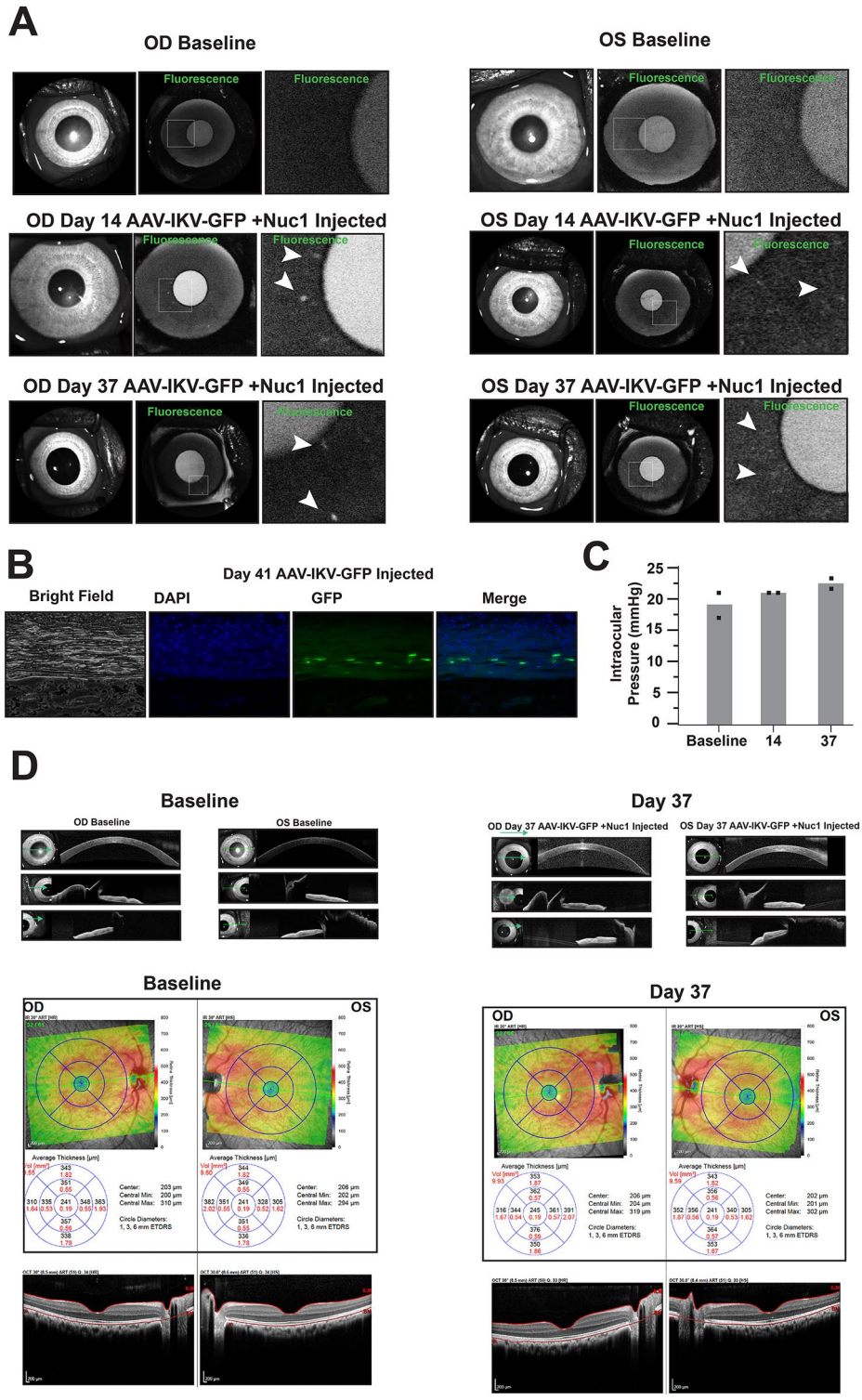

modeling a key feature of glaucoma and IAG. Furthermore, we have shown that AAV-IKV delivered decorin to the anterior segment reduces the elevated IOP, fibrosis and retinal ganglion cell death that is associated with TGFβ2 mediated pathophysiology in mice, suggestive of use of decorin as a potential therapy for glaucoma and IAG. A key limitation of our study is that it is performed in mice. As a first step towards preclinical studies in NHP, we have shown that a non-GMP grade AAV-IKV-GFP construct combined with Nuc1 is relatively safe in the NHP eye.

Several investigators have previously shown that intracameral injection of AAV expressing GFP can lead to transduction of corneal endothelium, stroma and/or trabecular meshwork[33–37]. In general, it was found that self-complementary AAV vectors performed significantly better than single-stranded genomes[38]. In our studies, we utilized a single stranded AAV. While self-complementary AAV genomes bypass second strand synthesis to enhance transgene expression, they are limited in capacity of the transgene expression cassette to half that of normal i.e. approximately 2.2Kb instead of 4.8Kb[39,40].

◀**Fig. 7**. AAV-IKV Mediated Gene Delivery to the Non Human Primate Cornea. (**A**) GFP expression in the eyes of live African green monkey (*Chlorocebus sabaeus*) at baseline, day 14 and day 37 post intracameral injection of AAV-IKV-GFP + Nuc1 in the *oculus dexter* (OD, right eye) and *oculus sinister* (OS, left eye). Whereas there was no detectable GFP fluorescence prior to injection (baseline), at day 14 post injection there was clear evidence of GFP expression in the cornea in a punctate pattern of expression (e.g. arrowheads) in live animals. Images containing arrowheads are higher magnification of the boxed areas. At all time points, the cornea of both eyes exhibited transparency and lack of any significant signs of inflammation, suggesting that the research grade vector did not lead to any significant immune responses. (**B**) Frozen cryosections examined for expression of GFP at day 45 post injection revealed GFP-positive cells in the cornea. (**C**) Intraocular pressure of AAV-IKV-GFP + Nuc1 injected eyes was similar to baseline at day 14 and 37 post injection. (**D**) High resolution OCT imaging of cornea, sclera and anterior chamber angles of AAV-IKV-GFP injected eyes at day 14 and day 37 were similar to baseline (**B**). Volume scans revealed an average thickness of the retina at day 14 and 37 was similar to baseline (**C**). High resolution OCT imaging of retina of AAV-IKV-GFP injected eyes at day 37 was also similar to baseline. See Supplementary Fig. 2 for day 14.

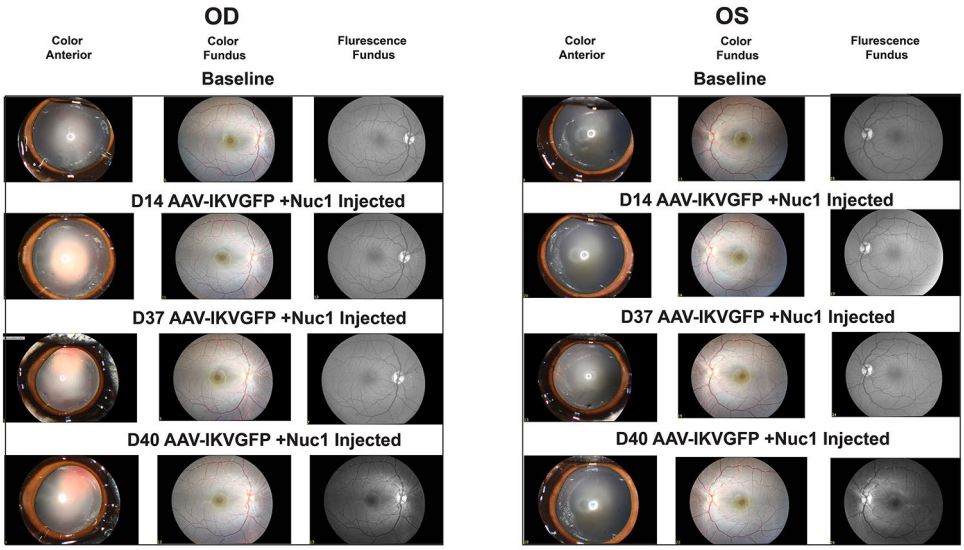

Fig. 8. AAV-IKV Mediated Gene Delivery to the Non Human Primate Cornea. Anterior color, Fundus color and fluorescence images of AAV-IKV-GFP + Nuc1 injected NHP eyes at day 14, 37 and 40 post injection. There is no evidence of GFP expression in the fundus at day 14 and 37 post injection. However, there is a minor GFP signal at day 40 post injection in both OS and OD.

Unexpectedly, we noted that intracameral injection of AAV-IKV could lead to GFP-positive corneal nerves. To our knowledge, corneal nerves have not been previously shown to be infected by any serotype of AAV despite these nerves being a significant target for gene therapy. The cornea is one of the most densely innervated tissues of the body, containing primarily sensory innervation[41]. Corneal nerves form a subbasal plexus underneath the epithelium, which extends thin nerve leashes containing nociceptors present at the surface of the cornea that could be observed in our studies[42]. These nerves are responsible for the sensations of touch, pain and temperature. The trophic properties of corneal nerves are necessary to maintain a healthy ocular surface. Disruption of the corneal nerves has been found to impair corneal healing[43]. Furthermore, diseases such as herpetic viral infections and ophthalmic surgical procedures cause corneal nerve disruption that can cause a range of conditions from mild dry eye to severe neurotrophic keratitis with corneal melting[44]. While not a focus of this study, AAV-IKV may be useful for the delivery of genes to corneal nerves, a field that has not yet been explored.

TGFβ2 is produced as a latent 390-amino acid precursor that forms dimers through association of its N-terminal latency-associated peptide (LAP). Dimeric, mature, biologically active C-terminal 112-amino acid TGFβ2 is generated from the cleavage and dissociation of LAP. However, mutations introduced into the LAP domain result in a constitutively active TGFβ2 peptide. Previously, it has been shown that constitutively active TGFβ2 expressed from an adenovirus vector injected intracamerally into rodents leads to an increase in IOP[26]. However, adenovirus vectors are known to cause significant inflammation, that ultimately causes a reduction in transgene expression. The immune responses associated with adenovirus are likely to significantly confound the phenotypic impact from elevated expression of TGFβ2. For these and additional reasons, we utilized AAV vectors in our studies, notwithstanding that Nuc1 peptide may be immunogenic, but we did not note any significant inflammation in mice or NHP in our studies. Indeed, AAV has been consistently described as a relatively benign vector that does not cause significant inflammation in the eye relative to adenovirus. However, since an empty AAV vector, i.e. AAV-IKV-pA also led to some mild fibrosis and elevation of TGFβ2 expression in our studies, AAV was not completely benign. However, the levels of elevated TGFβ2 and fibrosis from AAV-IKV were not

sufficient to cause an increase in IOP. Moreover, in our studies we utilized research grade AAV vectors and whether similar outcomes would be observed when using GMP grade vectors remains to be determined in future studies. In the context of clinical use, only the safety of AAV-IKV-Decorin and Nuc1 would be relevant.

Relative to humans, the murine lens occupies a very large volume of the eye. Consequently, intravitreal injections in mice sometimes result in damage to the lens epithelium. Incidentally, we noticed that in such animals there was a significant elevation of TGFβ2 in the lens epithelial cells (Supplementary Fig. 3A). In some animals, the lens epithelial cells formed a mass of cells on the surface of the lens (Supplementary Fig. 3B) and we hypothesize that such cells may migrate to the trabecular meshwork following lensectomy in IAG, resulting in fibrosis at the trabecular meshwork and increased IOP as discussed in detail previously[21]. In comparison to humans, the mouse lens occupies a very large volume of the eye and thus performing a lensectomy in mice to model IAG is technically challenging.

Onset of transgene expression from AAV-IKV was rapid, with IOP increasing in AAV-IKV-TGFβ2^{CS} injected animals within days and elevated IOP was maintained out to day 44 post-injection, the latest time point examined in this study. The increase in IOP was dependent upon the dose of AAV-IKV-TGFβ2^{CS} injected into animals.

Although generation of an animal model of glaucoma in NHPs is beyond the scope of the current study, we did find evidence that AAV-IKV-GFP can infect NHP cornea following intracameral injection. We found clear evidence of GFP fluorescence in live animals as well as in cryosections in both the the AAV-IKV-GFP injected eyes at day 14 and day 37 post injection, the latest time point examined. At all time points, the cornea of both eyes exhibited transparency similar to baseline and without any sign of inflammation, suggesting that the research grade vector did not lead to any significant immune responses. Furthermore, the IOP in AAV-IKV-GFP injected eyes did not differ significantly from baseline and similarly, anterior OCT images of AAV-IKV-GFP injected eyes at all time points were similar to baseline. Finally, volume scans of macula, blue laser autofluorescence wide-field images and all other clinical parameters in AAV-IKV-GFP injected eyes were found to be similar to baseline, indicating that AAV-IKV-GFP satisfies the initial criteria for further investigation as a candidate AAV for development of a gene therapy for glaucoma.

A limitation of our study is that while AAV-IKV-Decorin could inhibit AAV-IKV- TGFβ2^{CS} increase in IOP, fibrosis and ganglion cell death, our studies do not address whether pre-established IOP and fibrosis can be reversed. In order to conduct such a study, one would need to conduct multiple injections at different time points in the mouse eye. Such studies are technically challenging due to the small eyes of mice. Alternatively, one may develop an AAV-IKV- TGFβ2^{CS} where the transgene can be turned off after the observation of pathology and such mice subsequently injected with AAV-IKV-Decorin. Such studies are contemplated and beyond the scope of the current study.

Future studies will also examine the long-term consequences of elevated expression of decorin in the eye but given that decorin is naturally expressed in the eye in multiple tissues[23]and that recombinant decorin has previously been injected into human eyes[45] without any negative consequences, the approach described in this study deserves further evaluation as a potential gene therapy for glaucoma.

Data availability

Data is provided within the manuscript and supplementary information files. Additional details are available by contacting Rajendra.Kumar-Singh@tufts.edu.

Received: 15 August 2024; Accepted: 26 February 2025
Published online: 07 March 2025

References

1. Tham, Y. C. et al. Global prevalence of glaucoma and projections of glaucoma burden through 2040: a systematic review and meta-analysis. *Ophthalmology***121**, 2081–2090. https://doi.org/10.1016/j.ophtha.2014.05.013 (2014).
2. Foster, A. & Gilbert, C. Cataract in children. *Acta Paediatr.***92**, 1376–1378. https://doi.org/10.1080/08035250310007556 (2003).
3. Khan, A. O. & Al-Dahmash, S. Age at the time of cataract surgery and relative risk for Aphakic glaucoma in nontraumatic infantile cataract. *J. AAPOS.* **13**, 166–169. https://doi.org/10.1016/j.jaapos.2008.10.020 (2009).
4. Kountouras, J., Zavos, C. & Deretzi, G. Primary open-angle glaucoma. *N Engl. J. Med.***360**, 2679 (2009). author reply 2679–2680.
5. Weinreb, R. N., Aung, T. & Medeiros, F. A. The pathophysiology and treatment of glaucoma: a review. *JAMA***311**, 1901–1911. https://doi.org/10.1001/jama.2014.3192 (2014).
6. Kaufman, P. L., Mohr, M. E., Riccomini, S. P. & Rasmussen, C. A. Glaucoma drugs in the pipeline. *Asia Pac. J. Ophthalmol. (Phila).* **7**, 345–351. https://doi.org/10.22608/APO.2018298 (2018).
7. Lusthaus, J. A. & Goldberg, I. Investigational and experimental drugs for intraocular pressure reduction in ocular hypertension and glaucoma. *Expert Opin. Investig. Drugs.* **25**, 1201–1208. https://doi.org/10.1080/13543784.2016.1223042 (2016).
8. Gemenetzi, M., Yang, Y. & Lotery, A. J. Current concepts on primary open-angle glaucoma genetics: a contribution to disease pathophysiology and future treatment. *Eye (Lond).* **26**, 355–369. https://doi.org/10.1038/eye.2011.309 (2012).
9. Tripathi, R. C., Li, J., Chan, W. F. & Tripathi, B. J. Aqueous humor in glaucomatous eyes contains an increased level of TGF-beta 2. *Exp. Eye Res.***59**, 723–727. https://doi.org/10.1006/exer.1994.1158 (1994).
10. Inatani, M. et al. Transforming growth factor-beta 2 levels in aqueous humor of glaucomatous eyes. *Graefes Arch. Clin. Exp. Ophthalmol.***239**, 109–113. https://doi.org/10.1007/s004170000241 (2001).
11. Picht, G., Welge-Luessen, U., Grehn, F. & Lutjen-Drecoll, E. Transforming growth factor beta 2 levels in the aqueous humor in different types of glaucoma and the relation to filtering bleb development. *Graefes Arch. Clin. Exp. Ophthalmol.***239**, 199–207. https://doi.org/10.1007/s004170000252 (2001).
12. Ochiai, Y. & Ochiai, H. Higher concentration of transforming growth factor-beta in aqueous humor of glaucomatous eyes and diabetic eyes. *Jpn J. Ophthalmol.***46**, 249–253. https://doi.org/10.1016/s0021-5155(01)00523-8 (2002).
13. Ozcan, A. A., Ozdemir, N. & Canataroglu, A. The aqueous levels of TGF-beta2 in patients with glaucoma. *Int. Ophthalmol.***25**, 19–22. https://doi.org/10.1023/b:inte.0000018524.48581.79 (2004).
14. NikhalaShree, S. et al. Lowered decorin with aberrant extracellular matrix remodeling in aqueous humor and Tenon's tissue from primary Glaucoma patients. *Invest. Ophthalmol. Vis. Sci.***60**, 4661–4669. https://doi.org/10.1167/iovs.19-27091 (2019).

15. Min, S. H., Lee, T. I., Chung, Y. S. & Kim, H. K. Transforming growth factor-beta levels in human aqueous humor of glaucomatous, diabetic and uveitic eyes. *Korean J. Ophthalmol.***20**, 162–165. https://doi.org/10.3341/kjo.2006.20.3.162 (2006).
16. Jampel, H. D., Roche, N., Stark, W. J. & Roberts, A. B. Transforming growth factor-beta in human aqueous humor. *Curr. Eye Res.***9**, 963–969. https://doi.org/10.3109/02713689009069932 (1990).
17. Agarwal, P., Daher, A. M. & Agarwal, R. Aqueous humor TGF-beta2 levels in patients with open-angle glaucoma: A meta-analysis. *Mol. Vis.***21**, 612–620 (2015).
18. Sisto, M., Ribatti, D. & Lisi, S. Organ Fibrosis and Autoimmunity: The Role of Inflammation in TGFbeta-Dependent EMT. *Biomolecules* 11, (2021). https://doi.org/10.3390/biom11020310
19. Das, V., Bhattacharya, S., Chikkaputtaiah, C., Hazra, S. & Pal, M. The basics of epithelial-mesenchymal transition (EMT): A study from a structure, dynamics, and functional perspective. *J. Cell. Physiol.*https://doi.org/10.1002/jcp.28160 (2019).
20. Michael, I., Walton, D. S. & Levenberg, S. Infantile Aphakic glaucoma: a proposed etiologic role of IL-4 and VEGF. *J. Pediatr. Ophthalmol. Strabismus*. **48**, 98–107. https://doi.org/10.3928/01913913-20100518-04 (2011).
21. Yeung, H. H., Kumar-Singh, R. & Walton, D. S. Infantile Aphakic glaucoma: A proposed mechanism. *J. Pediatr. Ophthalmol. Strabismus*. **59**, 236–242. https://doi.org/10.3928/01913913-20210929-02 (2022).
22. Neill, T., Schaefer, L. & Iozzo, R. V. Decorin: a guardian from the matrix. *Am. J. Pathol.***181**, 380–387. https://doi.org/10.1016/j.ajpath.2012.04.029 (2012).
23. Schneider, M. et al. A novel ocular function for decorin in the aqueous humor outflow. *Matrix Biol.*https://doi.org/10.1016/j.matbio.2021.02.002 (2021).
24. Nikhalashree, S. et al. Anti-glaucoma medications Lowered decorin and altered profibrotic proteins in human Tenon's fibroblasts. *Exp. Eye Res.***224**, 109199. https://doi.org/10.1016/j.exer.2022.109199 (2022).
25. Hill, L. J. et al. Decorin reduces intraocular pressure and retinal ganglion cell loss in rodents through fibrolysis of the scarred trabecular meshwork. *Invest. Ophthalmol. Vis. Sci.***56**, 3743–3757. https://doi.org/10.1167/iovs.14-15622 (2015).
26. Shepard, A. R. et al. Adenoviral gene transfer of active human transforming growth factor-{beta}2 elevates intraocular pressure and reduces outflow facility in rodent eyes. *Invest. Ophthalmol. Vis. Sci.***51**, 2067–2076. https://doi.org/10.1167/iovs.09-4567 (2010).
27. Agrahari, V. et al. A comprehensive insight on ocular pharmacokinetics. *Drug Deliv Transl Res.***6**, 735–754. https://doi.org/10.1007/s13346-016-0339-2 (2016).
28. Vaajanen, A. & Vapaatalo, H. A single drop in the Eye - Effects on the whole body?? *Open. Ophthalmol. J.***11**, 305–314. https://doi.org/10.2174/1874364101711010305 (2017).
29. Almasieh, M. & Levin, L. A. Neuroprotection in glaucoma: animal models and clinical trials. *Annu. Rev. Vis. Sci.***3**, 91–120. https://doi.org/10.1146/annurev-vision-102016-061422 (2017).
30. Kumar, B., Mishra, M., Cashman, S. & Kumar-Singh, R. Retinal Penetrating Adeno-Associated Virus. *Invest Ophthalmol Vis Sci* In press, (2024). https://doi.org/10.1167/iovs.65.8.31
31. Kumar, B., Mishra, M., Talreja, D., Cashman, S. & Kumar-Singh, R. Cell-Penetrating chaperone Nuc1 for Small- and Large-Molecule delivery into retinal cells and tissues. *Invest. Ophthalmol. Vis. Sci.***65**, 31. https://doi.org/10.1167/iovs.65.8.31 (2024).
32. Maeda, A. et al. Circadian intraocular pressure rhythm is generated by clock genes. *Invest. Ophthalmol. Vis. Sci.***47**, 4050–4052. https://doi.org/10.1167/iovs.06-0183 (2006).
33. Rodriguez-Estevez, L., Asokan, P. & Borras, T. Transduction optimization of AAV vectors for human gene therapy of glaucoma and their reversed cell entry characteristics. *Gene Ther.***27**, 127–142. https://doi.org/10.1038/s41434-019-0105-4 (2020).
34. Frederick, A. et al. Engineered capsids for efficient gene delivery to the retina and cornea. *Hum. Gene Ther.***31**, 756–774. https://doi.org/10.1089/hum.2020.070 (2020).
35. Wang, L., Xiao, R., Andres-Mateos, E. & Vandenberghe, L. H. Single stranded adeno-associated virus achieves efficient gene transfer to anterior segment in the mouse eye. *PLoS One*. **12**, e0182473. https://doi.org/10.1371/journal.pone.0182473 (2017).
36. Bogner, B. et al. Capsid mutated Adeno-Associated virus delivered to the anterior chamber results in efficient transduction of trabecular meshwork in mouse and rat. *PLoS One*. **10**, e0128759. https://doi.org/10.1371/journal.pone.0128759 (2015).
37. Kong, F. et al. Self-complementary AAV5 vector facilitates quicker transgene expression in photoreceptor and retinal pigment epithelial cells of normal mouse. *Exp. Eye Res.***90**, 546–554. https://doi.org/10.1016/j.exer.2010.01.011 (2010).
38. Buie, L. K. et al. Self-complementary AAV virus (scAAV) safe and long-term gene transfer in the trabecular meshwork of living rats and monkeys. *Invest. Ophthalmol. Vis. Sci.***51**, 236–248. https://doi.org/10.1167/iovs.09-3847 (2010).
39. McCarty, D. M. Self-complementary AAV vectors; advances and applications. *Mol. Ther.***16**, 1648–1656. https://doi.org/10.1038/mt.2008.171 (2008).
40. McCarty, D. M., Monahan, P. E. & Samulski, R. J. Self-complementary Recombinant adeno-associated virus (scAAV) vectors promote efficient transduction independently of DNA synthesis. *Gene Ther.***8**, 1248–1254. https://doi.org/10.1038/sj.gt.3301514 (2001).
41. Marfurt, C. F. & Ellis, L. C. Immunohistochemical localization of tyrosine hydroxylase in corneal nerves. *J. Comp. Neurol.***336**, 517–531. https://doi.org/10.1002/cne.903360405 (1993).
42. Lazarov, N. E. Comparative analysis of the chemical neuroanatomy of the mammalian trigeminal ganglion and mesencephalic trigeminal nucleus. *Prog Neurobiol.***66**, 19–59. https://doi.org/10.1016/s0301-0082(01)00021-1 (2002).
43. Murphy, C. J. et al. Spontaneous chronic corneal epithelial defects (SCCED) in dogs: clinical features, innervation, and effect of topical SP, with or without IGF-1. *Invest. Ophthalmol. Vis. Sci.***42**, 2252–2261 (2001).
44. Wilson, S. E. & Ambrosio, R. Laser in situ keratomileusis-induced neurotrophic epitheliopathy. *Am. J. Ophthalmol.***132**, 405–406. https://doi.org/10.1016/s0002-9394(01)00995-3 (2001).
45. Abdullatif, A. M. et al. Intravitreal decorin preventing proliferative vitreoretinopathy in perforating injuries: a pilot study. *Graefes Arch. Clin. Exp. Ophthalmol.***256**, 2473–2481. https://doi.org/10.1007/s00417-018-4105-7 (2018).

Acknowledgements

This study was funded by the Children's Glaucoma Foundation. We are grateful to Dr. Deepa Talreja for providing technical support.

Author contributions

PR and MM were responsible for generating the data presented in Figs. 1, 2, 3, 4, 5 and 6. Figures 7 and 8 describing non-human primate data were generated by RK-S with the studies being performed under contract at St. Kitts Biomedical Research Organization in West Indies. RK-S and DW were responsible for overall project design, acquiring funding and writing the manuscript. SC was responsible for project design and assistance in writing the manuscript. All authors reviewed the manuscript.

Funding

This study was funded by the Children's Glaucoma Foundation

Declarations

Competing interests
The authors declare no competing interests.

Additional information
Supplementary Information The online version contains supplementary material available at https://doi.org/10.1038/s41598-025-92273-5.

Correspondence and requests for materials should be addressed to R.K.-S.

Reprints and permissions information is available at www.nature.com/reprints.

Publisher's note Springer Nature remains neutral with regard to jurisdictional claims in published maps and institutional affiliations.